# Structural and magnetic susceptibility characterization of Pu(V) aqua ion using sonochemistry as a facile synthesis method

Dalodiere, E.; Virot, M.; Dumas, T.; Guillaumont, D.; Illy, M.; Berthon, C.; Guerin, L.; Rossberg, A.; Venault, L.; Moisy, P.; Nikitenko, S.;

Originally published:

October 2017

**Inorganic Chemistry Frontiers 5(2018), 100-111**

DOI: https://doi.org/10.1039/C7QI00389G

Perma-Link to Publication Repository of HZDR:

https://www.hzdr.de/publications/Publ-28420

View Article Online
DOI: 10.1039/C7QI00389G

# Structural and Magnetic Susceptibility Characterizations of Pu(V) Aqua Ion using Sonochemistry as a Facile Synthesis Method

Elodie Dalodière[1], Matthieu Virot[1,*], Thomas Dumas[2], Dominique Guillaumont[2], Marie-Claire Illy[2], Claude Berthon[2], Laëtitia Guerin[2], André Rossberg[3], Laurent Venault[2], Philippe Moisy[2], Sergey I. Nikitenko[1]

[1] Université de Montpellier, Institut de Chimie Séparative de Marcoule (ICSM), UMR 5257, CEA-CNRS-UM-ENSCM, Site de Marcoule, BP17171, 30207 Bagnols sur Cèze, France.
[2] French Nuclear and Alternative Energies Commission CEA Nuclear Energy Division – CEA Marcoule Research Department of Mining and Fuel Recycling ProCesses (DMRC)- Site de Marcoule, BP17171, 30207 Bagnols sur Cèze, France.
[3] Helmholtz-Zentrum Dresden - Rossendorf, Institute of Resource Ecology, Bautzner Landstraße 400, 01328 Dresden, Germany.

*matthieu.virot@cea.fr





**Abstract**

Due to its potential contribution in the environmental migration of actinides, Pu(V) gained much more attention since the past few years. However, the preparation of concentrated (up to mM) and pure Pu(V) solutions is quite difficult and often hindered by its great instability towards disproportionation thus limiting the accessibility to physical and chemical property data. This work describes the rapid and facile sonochemical preparation of relatively stable Pu(V) solutions at the millimolar range free from the admixtures of other oxidation states of plutonium. The mechanism deals with the sonochemical reduction of Pu(VI) in weakly acid perchloric solutions by the in situ generated $H_2O_2$ which kinetics can be dramatically enhanced under high frequency ultrasound and $Ar/O_2$ atmosphere. The quasi-exclusive presence of the Pu(V) aqua ion in solution was evidenced by UV-Vis absorption spectroscopy. The prepared solutions were found to be stable for more than one month which allowed accurate XAFS and NMR investigations of Pu(V). EXAFS spectra revealed the presence of two trans dioxo Pu=O bonds at 1.81 Å and 4-6 equatorial Pu-$O_{eq}$ interactions at 2.47 Å characteristic from coordinated water molecules. The exact number of water molecules ($N[O_{eq}(H_2O)] = 4$) was determined by simulating EXAFS spectra of $PuO_2^+$ aqua complex using DFT calculations (geometry and Debye-Waller factor) and comparing them with experimental signals. For the first time, the magnetic susceptibility of the pentavalent state of plutonium in aqueous solution was also determined ($\chi_M = 16.3\ 10^{-9}\ m^3\ mol^{-1}$ at 25°C) and the related Curie constant was estimated ($C = 6.896\ 10^{-6}\ m^3\ K\ mol^{-1}$).

View Article Online
DOI: 10.1039/C7QI00389G



## 1. Introduction

In acidic aqueous solutions, plutonium exhibits the extraordinary ability to coexist within four oxidation states from +III to +VI. The relative abundance of each oxidation state is highly dependent upon the Pu concentration, pH, presence of complexing agents and ionic strength, and redox potential.[1-3] Tetravalent plutonium, which is the most stable oxidation state in acidic media under aerobic atmosphere, in combination to trivalent and hexavalent states, have been extensively studied particularly for the development of Pu separation processes.[2, 3] Investigations devoted to Pu(V) solutions have been however poorly reported in the literature despite the fact that researches carried out on the pentavalent state have been more referenced from the 1990s when the behaviour of Pu and its interaction with the environment gained more importance. The subsurface mobility of Pu(V) is indeed predicted to be much higher in comparison to the other oxidation states.[4-9] However, the pentavalent state of Pu is highly prone to disproportionation even in moderately acidic solutions. As a function of the presence of the other oxidation states in the solutions, several disproportionation mechanisms have been proposed in the literature (reactions (1-2), the first favoured at very low concentrations of Pu(III)).[10, 11]

$$2\ PuO_2^{+} + 4\ H^{+} \leftrightharpoons Pu^{4+} + PuO_2^{2+} + 2\ H_2O \quad (1)$$

$$3\ PuO_2^{+} + 4\ H^{+} \leftrightharpoons Pu^{3+} + 2\ PuO_2^{2+} + 2\ H_2O \quad (2)$$

Both reactions show a strong dependency of Pu(V) disproportionation against $H^+$ concentration thus driving the preparation of Pu(V) in acid solutions quite tricky, but also confirming the higher stability of Pu(V) in geochemical context where near neutral conditions dominate.[5, 6, 9] Pu(V) reactivity appears in addition strongly dependent upon its concentration, the radiolysis, and the presence of other Pu oxidation states due to the closeness of the standard redox potentials of Pu couples. Principally, the reported preparations of Pu(V) solutions deals with electrochemical or separation/extraction methods, and are generally carried out at low concentration ($10^{-5}$ - $10^{-10}$ M) and pH > 3.[9, 12, 13] Recently, some authors reported the use of ozone to prepare pure Pu(V) solutions in relatively low concentration (2 $10^{-8}$ M).[14] Ozone bubbling into a Pu(IV) solution induces its almost total conversion into a mixture composed of Pu(V) and Pu(VI) which then slowly converts to Pu(V) which kinetics can be improved by increasing the pH in the 3-7 range. In these conditions, Pu(V) remains stable for more than one month and the solution has the advantage to be quickly prepared without residual oxidants or organic solvents that can hinder further investigations. The preparation of large volumes and more concentrated solutions of Pu(V) is much more complex and poorly reported in the literature thus hindering the determination of physical and chemical data from experimental solutions. Cohen *et al.* nevertheless reported the preparation of a 0.02 M Pu(V) solution by electrolytic reduction of Pu(VI) at a potential of about 0.54 V (vs SCE) in 0.2 M $HClO_4$.[2, 15] Rabideau et *al.* described the addition of a neutral sodium iodine solution to plutonyl solution.[16] The protocol required carefully selected conditions with a final solution only composed of 25 to 50% of Pu(V).

Probing the magnetic properties of the actinide ions is very important to predict and characterize their interaction with ligands in solution.[17, 18] Up to our knowledge, the magnetic susceptibility of the pentavalent state of Pu has never been investigated in aqueous solution. Nevertheless, we can note that some authors provided a value in 1944 by means of the Gouy method.[10] The studied Pu(V) solution was however not pure and its concentration was changing with time. Otherwise, only a few studies investigated the characterization of the structure of the Pu(V) aqua ion with XAFS (X-ray

View Article Online
DOI: 10.1039/C7QI00389G

absorption fine structure) techniques.[19-23] Although there is an agreement concerning the presence and distance attributed to the two dioxo bonds, the exact number of water molecules coordinating Pu(V) aqua ion in the equatorial plane still suffer from experimental confirmation.[19-23] Such knowledge is highly important to predict the behaviour, complexation, and reactivity of the pentavalent state which is particularly under current focus due to Pu migration concern. Generally, the few experimental investigations dedicated to the solvation environment of $PuO_2^+$ agree for the predominance of four water molecules in the equatorial plane in non-complexing aqueous media,[20-22, 24] although the penta-aqua complex has also often been predicted with theoretical calculations to be the most favourable structure.[25-27] The interpretation of the results with XAFS techniques is however highly function of the parameter settings and often combined with a debatable precision.[24, 28] More recently, computational studies dedicated to the solvation environment of actinide species concluded that the predominant $PuO_2^+$ complex is probably coordinated by four water ligands.[29, 30]

Historically, hydrogen peroxide has been a very important reagent in actinide chemistry and the related industrial processes for purification or separation purposes (U, Pu and Np).[2, 31-34] Generally, this salt free reagent avoids large dilution of solutions and generates gaseous by-products without any formation of solution impurities. At the lab scale, $H_2O_2$ is often used in nitric media to reduce Pu(VI) into Pu(V) which then disproportionates and allows the generation of stable Pu(IV) solutions in agreement with the reactions (1-2). Further addition of hydrogen peroxide can lead to the formation of Pu(III) or a mixture of Pu(IV) and Pu(III) depending on the experimental conditions (temperature, acidity, concentration, presence of complexing ligands, etc.). $O_2/H_2O_2$ ($E° = 0.695$ V/SHE) or $H_2O_2/H_2O$ ($E° = 1.763$ V/SHE)[35] couples are indeed able to respectively reduce Pu(IV), or oxidize Pu(III) (reactions (3-4)). The addition of $H_2O_2$ during Pu oxidation state stabilizations is therefore delicate and should be used with parsimony to avoid mixtures of Pu oxidation states. In less acidic conditions, studies related to Pu(VI) reduction with $H_2O_2$ are really scarce but it is interesting to note that some authors described the detection of Pu(V) during the whole reduction process into Pu(IV) in 0.5 M $HNO_3$.[36]

$$2\ Pu^{4+} + H_2O_2 \leftrightharpoons 2\ Pu^{3+} + O_2 + 2\ H^+ \quad (3)$$

$$2\ Pu^{3+} + H_2O_2 + 2\ H^+ \leftrightharpoons 2\ Pu^{4+} + 2\ H_2O \quad (4)$$

Sonochemistry has attracted considerable attention as a potentially "reagent-free" route to control the oxidation states of actinide ions during spent nuclear fuel reprocessing, mostly due to the *in situ* generation of hydrogen peroxide and/or nitrous acid during the sonication of aqueous nitric solutions.[37, 38] In pure water saturated with noble gases, power ultrasound causes the homolytic splitting of $H_2O$ molecules yielding $H^\cdot$ and $OH^\cdot$ radicals (reaction (5), ")))" is for a reaction initiated under ultrasound).[39-43] These highly reactive species mostly recombine into $H_2O$ inside the cavitation bubble,[42, 43] some $OH^\cdot$ radicals (roughly 20%)[43, 44] can nevertheless diffuse to the bubble interface where the temperatures are lower and recombine into hydrogen peroxide (reaction (6)). Molecular hydrogen $H_2$ is formed as a recombination product of $H^\cdot$ radicals mostly in the gaseous phase of the collapsing bubble (reaction (7)).[42, 45] Several investigations devoted to the kinetics of $H_2O_2$ sonochemical formation have been reported in the literature.[46-50] It was showed that $H_2O_2$ formation rate in pure water can be significantly enhanced when increasing the ultrasound frequency or when using a mixture of $Ar/O_2$ as a saturating atmosphere.[48, 49, 51] Experimentations showed that higher yields were observed under $Ar/(20\text{-}30\ vol.\%)O_2$ gas atmosphere and were attributed to the generation of both $OH^\cdot$ and $HO_2^\cdot$ species as a result of $O_2$ reactivity or dissociation in the cavitation bubbles (reactions (8-12)).[38, 49, 52]

View Article Online
DOI: 10.1039/C7QI00389G

$$H_2O \rightarrow))) \rightarrow H^{\cdot} + OH^{\cdot} \quad (5)$$

$$2\ OH^{\cdot} \rightarrow H_2O_2 \quad (6)$$

$$2\ H^{\cdot} \rightarrow H_2 \quad (7)$$

$$H^{\cdot} + O_2 \rightarrow HO_2^{\cdot} \quad (8)$$

$$2\ HO_2^{\cdot} \rightarrow H_2O_2 + O_2 \quad (9)$$

$$O_2 \rightarrow))) \rightarrow 2\ {}^{\cdot}O^{\cdot} \quad (10)$$

$${}^{\cdot}O^{\cdot} + HO^{\cdot} \rightarrow HO_2^{\cdot} \quad (11)$$

$${}^{\cdot}O^{\cdot} + H_2O \rightarrow HO^{\cdot} + HO^{\cdot} \quad (12)$$

This work can be divided in three distinctive parts focusing on (i) the preparation and study towards aging of concentrated and relatively stable Pu(V) solutions under ultrasound irradiation at room temperature; (ii) the evidence of the exclusive or quasi-exclusive presence of the pentavalent state in the prepared solutions followed by its structural characterization by XAFS and computational techniques; (iii) the determination of the magnetic susceptibility of Pu(V) by NMR.

View Article Online
DOI: 10.1039/C7QI00389G

## 2. Experimental

***Caution!*** *Pu is an α-emitting element presenting serious health risks. Studies dealing with such an element require a careful handling coupled with appropriate infrastructures and trained workers.*

### 2.1. Materials

Stock solution were purified in agreement with the previously described procedure.[38] Pu isotopy consisted in a mixture of 96.90% $^{239}$Pu, 2.99% $^{240}$Pu, 0.05% $^{241}$Pu, and 0.06% $^{242}$Pu. Reagents used in this study were all of analytical grade and were purchased from Sigma-Aldrich and VWR. Aqueous solutions were prepared with purified ultrapure water having a resistivity higher than 18.2 MΩ cm at 25°C. Experiments were performed under pure Ar (purity > 99.9%), Ar/$O_2$ (20 vol.% of $O_2$) or Ar/CO (10 vol.% of CO) atmospheres provided by Air Liquide.

### 2.2. Pu(VI) preparation

To prepare Pu(VI) solution, an aliquot of Pu(IV) initially stabilized in nitric acid was evaporated to almost dryness. Concentrated $HClO_4$ aliquot was then added and Pu(IV) was oxidized by heating until fuming perchloric acid followed by evaporation until a wet salt is obtained.[5] After dilution in pure water, the obtained orange solution was characterized by UV-vis absorption spectroscopy which showed a complete conversion of the Pu(IV) solution into Pu(VI) in agreement with the literature.[2] In general, the as prepared Pu(VI) solutions exhibit a good stability, however, some Pu(VI) self-irradiation reduction is observed after several weeks of storage. To avoid the formation of Pu mixture from self-irradiation, Pu(VI) solution was directly dilute to the appropriate concentration after synthesis and sonicated within the few days following its preparation.

### 2.3. Sonochemical experiments

Experiments with Pu were performed at the ATALANTE nuclear facility (Marcoule, CEA research centre, France) in a glove box under negative pressure. This glove box is equipped with two different sonochemical reactors. Experiments carried out at low frequency ultrasound (20 kHz) were performed with a 1 cm² titanium horn fitted on top of a 50 mL homemade reactor. Ultrasound was provided by a 750 W generator (Sonics & Materials VCX 750) connected from outside the glove box.[38] High frequency studies (203 kHz) were performed in a 250 mL cylindrical reactor with a 25 cm² transducer (L3 Communications ELAC Nautik) connected from the bottom of the cell to a 125 W generator situated outside the enclosure (LVG 60 RF-generator). For high frequency experiments, solution was stirred with a mechanical agitation in the meantime (at 240 rpm) to obtain a homogeneous distribution of the acoustic bubbles in the cell.[49] The specific absorbed acoustic power equal to 0.34 and 0.13 W mL$^{-1}$ for 20 and 203 kHz ultrasound respectively, was obtained by the conventional thermal probe method.[39] Both reactors are tight and supplied with several connections dedicated to gas bubbling, temperature control and aliquot sampling. The temperature was maintained at 21±1°C with a cryostat (Lauda Ecoline RE 210) during ultrasonic treatment and controlled with a thermocouple immersed into the sonicated solutions. The various treated solutions were sparged with gas (at a constant flow rate of 100 mL min$^{-1}$) which started 15 min before ultrasound triggering and was maintained into the solution during the whole experiment. The ratio of polyatomic gas to Ar results from previous investigations which showed optimized oxidant or reducing conditions with the selected gas mixtures.[49, 53]

View Article Online
DOI: 10.1039/C7QI00389G



## 2.4. UV-visible spectroscopy

During sonolysis, aliquots of solution (2 mL) were sampled at regular time intervals. At low frequency, aliquots were filtered with 0.2 µm PTFE filters to remove potential Ti particle contamination arising from the horn surface erosion (not required at 203 kHz where Ti erosion does not occur).[38, 54] Then, samples were analysed by UV–vis absorption spectrophotometry (Shimadzu UV3600 connected with optic fibres or Shimadzu UV3150 directly connected to the glove box) in 1 or 5 cm quartz cells. The concentration of Pu(VI) was followed at 830 nm ($\varepsilon$ = 533 $cm^{-1}$ $M^{-1}$) while Pu(V) was followed at 569 nm ($\varepsilon$ = 15 $cm^{-1}$ $M^{-1}$). "Peak-valley" differences in absorbance were measured to determine the concentration variations. Due to the spectrophotometer resolution, the narrow Pu(VI) peak at 830 nm was fitted with a Lorentzian function for the concentration calculations. The formation of $H_2O_2$ resulting from the homolytic dissociation of sonicated water molecules was measured by mixing the filtered sampled aliquots (1:1) with a 1.2 $10^{-2}$ M $TiOSO_4$ solution (0.330 g $TiOSO_4$ dissolved in 100 mL of pure water under stirring and previously gently heated in 3.5 mL of 18 M $H_2SO_4$) to form a colorimetric complex absorbing at 410 nm ($\varepsilon$ = 710 $cm^{-2}$ $M^{-1}$).[50] An external calibration curve was previously prepared with a $H_2O_2$ standard solution.

## 2.5. XAFS experiments

Pu $L_{III}$-edge XAFS measurements were performed at the European Synchrotron (ESRF, Grenoble, France) at the Rossendorf Beamline (BM20, ROBL)[55] which is equipped with a collimating and focusing mirror and a water cooled Si(111) double-crystal monochromator in order to reject higher order harmonics and monochromatize the incident white X-rays. The sample spectra were recorded in transmission mode by using $Ar/N_2$ filled ionization chambers, whereas the $Ar/N_2$ ratio was optimized for the measured energy range. The incident photon energy was calibrated *in situ* by measuring after the sample ($I_1/I_2$) the first derivative XANES (X-ray Absorption Near Edge Structure) spectrum of a Zr foil defined at 17998 eV. Experimental spectra were recorded at the Pu $L_{III}$ edge and the ionization energy ($E_0$) was preliminary defined at the maximum of the white line and varied as a free fit parameter. The energy range investigated for EXAFS (Extended X-ray Absorption Fine Structure) measurements was chosen depending on Pu content in the samples from 3.3 $Å^{-1}$ to 12.3 $Å^{-1}$. EXAFS data analyses were performed with Athena and Arthemis software from ifeffit package[56, 57] and theoretical scattering phases and amplitude functions were calculated by the *ab initio* FEFF8.4 code from hypothetical plutonyl structure.[58] All fitting operations were performed in R-space over individual radial distances: 2 $O_{yl}$ and several $O_{eq}(H_2O)$ with corresponding Debye-Weller factors ($\sigma^2$) for every considered distance in the first coordination shell.

## 2.6. Computational methods

Quantum chemical calculations were performed at the DFT level of theory using the B3LYP functional. The Stuttgart small-core relativistic effective core potential (RECP) and associated basis set was used for the actinide atom.[59-61] The 6-311+G(d,p) basis set was employed for other atoms. The DFT calculations were carried out using the Gaussian 09 software package.[62] Calculations were done in the presence of a continuum solvent model. The geometries of $PuO_2(H_2O)_4(H_2O)_8^+$ and $PuO_2(H_2O)_5(H_2O)_{10}^+$ complexes were optimized and characterized by harmonic frequency analysis as local minima. Several configurations were considered in the calculations corresponding to different arrangements of water molecules. The results are reported for the lowest energy configuration of each complex.

View Article Online
DOI: 10.1039/C7QI00389G



*Ab initio* EXAFS spectra were simulated using DFT structural parameters (bond distances and Debye-Waller factors) without any further fitting. Previously, we have shown that it is possible to reproduce accurately EXAFS experimental spectrum of actinides compounds by using such methodology.[63, 64] The EXAFS spectra were simulated with FEFF9 from DFT optimized structures and *ab initio* Debye-Waller factors for all multiple-scattering paths up to a half-path length of 6 Å. *Ab initio* Debye-Waller factors were calculated at 300 K for each scattering path from the dynamical matrix extracted from the DFT frequency calculation as implemented in FEFF9.[65, 66] The amplitude factor $S_0^2$ was fixed to 0.9 as in the EXAFS fitting procedure for the liquid samples. The geometries and vibrational frequencies of $PuO_2^+$ complex with four and five coordinated water molecules were optimized through DFT calculations and the corresponding thermal Debye-Waller factors were determined from the vibrational frequencies.[66]

The prerequisite condition to simulate correctly experimental EXAFS spectra from such calculations is that bond distances are accurately reproduced by the quantum chemical model. For this purpose, we have done preliminary calculations on the well characterized uranyl aqua ion. In aqueous solution, uranyl is known to be predominantly coordinated by five water molecules in the equatorial plane.[67] Previous DFT studies on uranyl ion have shown that the inclusion of an explicit second hydration shell improves the agreement with experimental data for structural parameters.[68, 69] In the present work, structural parameters were computed for actinyl complexes with first and second solvation shell water molecules. Solvent effects beyond the second hydration sphere were taken into account through a continuum model. The bond distances were calculated from DFT (B3LYP) for $UO_2(H_2O)_5(H_2O)_{10}^{2+}$ complex. The predicted U-$O_{yl}$ and U-$O_{eq}$ distances are equal to 1.773 Å and 2.445 Å, respectively, which is in close agreement with experimental values determined from EXAFS in aqueous solution (the reported values are ranging from 1.76 to 1.78 Å for the U-$O_{yl}$ distance and from 2.40 to 2.42 Å for the U-$O_{eq}$ distance).[70-73] The good agreement between experimental and calculated distances (within 0.04 Å) for uranyl aqua ion made us confident that structural parameters can be correctly reproduced for the $PuO_2^+$ ion by using the same approach.

## 2.7. Magnetic susceptibility

The molar magnetic susceptibility $\chi_M$ was calculated by the chemical shift difference $\Delta\delta$ measured between $^1$H NMR signal of working (t-BuOH in) and reference (t-BuOH out) solutions using the Evans method.[74] The shift ($\Delta\delta = \delta_{tBuOH+Pu(V)} - \delta_{tBuOH}$) observed on NMR signal is directly correlated to the magnetic susceptibility $\chi_M$ according to the equation (13). $^1$H NMR spectra of Pu(V) solutions were recorded using a 400 MHz Fourier transform spectrometer (Agilent DD2). Measurements were carried out at every 5° step in the 5-50°C temperature range. For some experiments, and to obtain a higher signal, Pu(V) solution was concentrated by evaporating the solution at room temperature under Ar bubbling overnight. A careful examination of the UV-Vis spectra confirmed the stability of the solution in the concentration range studied. The absence of modification of the spectra in the presence of t-BuOH was also confirmed. The solutions were directly analysed and UV-Vis spectra were measured again to confirm the absence of chemical transformation occurring during NMR analyses.

$$\chi_M = \frac{3\Delta\delta}{10^3[\mathrm{Pu(V)}]} \qquad (13)$$

where, $\Delta\delta$ represents the chemical shift difference between the reference and the working solution of *tert*-butanol signals, and $\chi_M$, the sample molar magnetic susceptibility ($m^3.mol^{-1}$).

View Article Online
DOI: 10.1039/C7QI00389G



## 3. Results and discussion

### 3.1. Pu(VI) sonolysis at high and low frequency ultrasound

The sonication of a 1.2 mM Pu(VI) aqueous solution under 203 kHz ultrasound and $Ar/O_2$ atmosphere leads to a significant decrease of its concentration which can be followed at 830 nm by UV-Vis absorption spectroscopy. The generation of Pu(V) is simultaneously observed with an absorption peak standing at 569 nm. The corresponding reduction kinetics is illustrated in Figure 1.a. where the almost total conversion of the initial Pu(VI) into Pu(V) can be observed in less than 3 h of sonication (yield >95%). Interestingly, the amount of residual Pu(VI) is found to decrease again when ultrasound stops: as expressed by the corresponding UV-vis spectra presented in Figure S1 (Supporting Information), less than 1% of Pu(VI) remains after roughly 2 h of storage. A pH solution drop from pH = 3.5 before sonication to pH = 2.8 after 160 min of sonication is also observed. Figure 1.b. illustrates the behaviour of a more concentrated aqueous solution of Pu(VI) (2.3 mM) sonicated at 203 kHz under $Ar/O_2$ atmosphere. The plotted curves agree with the previous observations reported for a lower concentration although the initial reduction rate is found to be much lower ($W_0(-Pu^{VI})$= 33.6 µmol $min^{-1}$ against 20.0 µmol $min^{-1}$ for the 1.2 mM and 2.3 mM solutions, respectively). Furthermore, the reduction of Pu(VI) also continues in the absence of ultrasound (US). The UV-Visible spectra of the 2.3 mM Pu solution before and after treatment are showed in Figure 2 with a 5 cm quartz cuvette in the case of Pu(V) solution which agree with the literature and evidence the high purity of the here prepared solution.[2, 10] The narrow peak at 569 nm results from electronic transitions within the 5f shell. The presence of a residual Pu(VI) amount estimated at 2.5 $10^{-5}$ M (less than 1% of the total content) can also be noted. Whatever the Pu concentration, the careful examination of the UV-Vis absorption spectra, in combination to the stability of the total Pu(VI) and Pu(V) content in the solution expressed by the green dots in Figure 1, suggests the absence of other Pu oxidation states in this system, specially Pu(III).

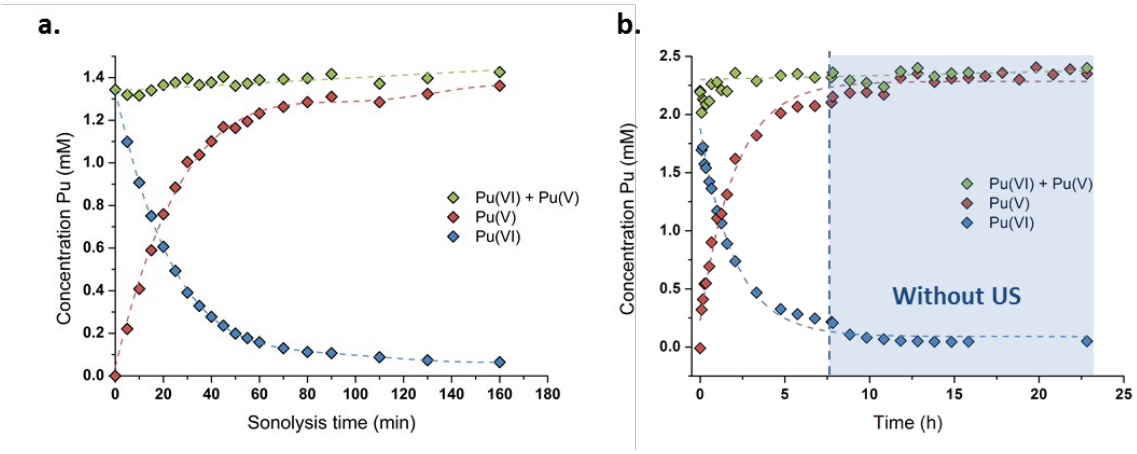


**Figure 1: Concentration evolutions for Pu(VI) and Pu(V) measured at 21°C under high frequency ultrasound (203 kHz, 0.13 W $mL^{-1}$, $Ar/(20\%)O_2$) for a (a.) 1.2 mM solution, and a (b.) 2.3 mM solution (" ⋮ " symbolizes ultrasound stop, the green data express the sum of the determined concentrations of Pu(VI) and Pu(V)).**

View Article Online
DOI: 10.1039/C7QI00389G



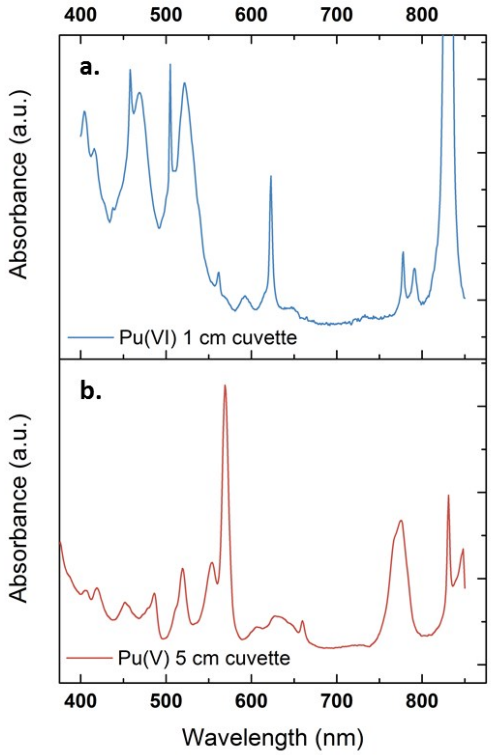


**Figure 2: UV-vis absorption spectra observed for a 2.3 mM aqueous Pu(VI) solution (a.) before, and (b.) after sonolysis (203 kHz, 0.13 W.mL$^{-1}$, 21°C, Ar/(20%)$O_2$). The residual content of Pu(VI) in the Pu(V) solution is approximately 1%. The final solution is devoid of other Pu oxidation states or species such as colloids or nitrate complexes. The obtained solution is light pink.**

Consistent observations were observed for similar conditions carried out under pure Ar atmosphere although kinetics evidenced a much lower reduction rate for Pu(VI) (Figure S2, Supporting Information). It is known that sonication allows the formation of $H_2O_2$ that can accumulate in aqueous solutions (reactions (5-6)).[42, 43] Pu(VI) reduction can therefore be explained by the in situ formation of $H_2O_2$ resulting from the sonochemical water molecule splitting and the subsequent recombination of the as-formed $OH^{\cdot}$ radicals (reaction (14)). Such a behaviour has been already reported during the 20 kHz sonication of nitric aqueous solutions of Pu(IV) or Pu(III) in the presence of anti-nitrous reagents.[38] The higher accumulation rates observed for Pu(V) under Ar/$O_2$ atmosphere can be explained by higher $H_2O_2$ yields in comparison to pure Ar.[50] This phenomenon is explained by the scavenging of $H^{\cdot}$ radicals with molecular $O_2$ inside the cavitation bubbles. This reaction avoids the recombination between $H^{\cdot}$ and $OH^{\cdot}$ radicals and generates hydroperoxyl radicals ($HO_2^{\cdot}$) which finally enhance $H_2O_2$ yields in agreement with the reactions (8-9).[75] $H_2O_2$ yields are also promoted by the dissociation of molecular oxygen inside the cavitation bubbles which is known to take place under high frequency ultrasound in agreement with the reactions (10-12).[50] The sonolytic overproduction of $H_2O_2$ can therefore enable to continue Pu(VI) reduction process when ultrasound stops (Figure 1.b. or Figure S1, Supporting Information).

$$2\ PuO_2^{2+} + H_2O_2 \rightarrow 2\ PuO_2^{+} + O_2 + 2\ H^{+} \qquad (14)$$

According to the literature, the reduction kinetic law for Pu(VI) in the presence of $H_2O_2$ is proportional to their respective initial concentrations and inversely proportional to the solution acidity (with k = 0.75 ± 0.1 min$^{-1}$ at 22°C (I = 1), equation (15)).[76, 77] The preparation of 2.3 mM Pu(VI)

View Article Online
DOI: 10.1039/C7QI00389G

solutions by dilution of the stock solution with pure water unavoidably increases the sonicated solution acidity in comparison to the 1 mM Pu(VI) solutions, and therefore explains the longer time required to reduce the Pu(VI) amount of the 2.3 mM Pu solution for a similar accumulation rate of $H_2O_2$ (Figure 1.a. vs. 1.b.).

$$-\frac{d[Pu(VI)]}{dt} = k\,\frac{[Pu(VI)][H_2O_2]}{[H^+]} \qquad (15)$$

The effect of the ultrasonic frequency towards reduction kinetics was investigated by sonicating Pu(VI) solutions at low frequency. In agreement with high frequency experiments, the 20 kHz sonolysis of a 1 mM Pu(VI) solution in water (pH = 3.6) under Ar or $Ar/O_2$ atmosphere leads to its UV-Vis absorption decrease at 830 nm and the simultaneous generation of Pu(V) absorbing at 569 nm as illustrated in Figure 3 and Figures S3 and S4 (Supporting Information, Ar atmosphere lowers the reduction rate in agreement with 203 kHz experiments).[2] The main difference lies in the Pu(VI) reduction rate which was found to be dramatically decreased at 20 kHz whatever the saturating atmosphere. Furthermore, the amount of Pu(VI) remaining after sonication (or one day after sonication) is higher than what observed under high frequency ultrasound (Figure S3, Supporting Information). The reduction kinetic differences can be explained by an increase of $H_2O_2$ yields at high frequency in aqueous solutions in comparison to low frequency ultrasound.[50] This higher formation rate is related to several phenomena occurring at high frequencies: (i) the increased number of cavitation bubbles,[78] (ii) the shortened ultrasound wave periods increasing the bubble surface-to-volume ratio (S/V) and leading to an enhanced rectified diffusion,[39, 79] and (iii) the higher intrabubble vibronic temperatures providing a higher dissociation degree of $O_2$.[49, 80] The measured $H_2O_2$ rate at low frequency in pure water saturated with $Ar/O_2$ was found to reach 2.8 ± 0.3 µM $min^{-1}$ which is much lower than what observed at 203 kHz, i.e 12.9 ± 1.5 µM $min^{-1}$. Under pure Ar, the 20 kHz formation rate reaches 1.1 ± 0.1 µM $min^{-1}$ whereas 2.1 ± 1.5 µM $min^{-1}$ are measured at high frequency.[50] Whatever the experimental conditions, the sonochemical yields of $H_2O_2$ were found to be dramatically reduced in the presence of Pu(VI). For instance, $H_2O_2$ formation rate reached only 0.6 mM at 203 kHz after 140 min of sonolysis whereas 1.8 mM is usually observed without Pu thus confirming again its contribution in the reduction process during and few hours after sonication. Note that the local heating generated at the bubble solution interface (few hundreds of degrees) may also favour a reaction kinetic increase.[54]

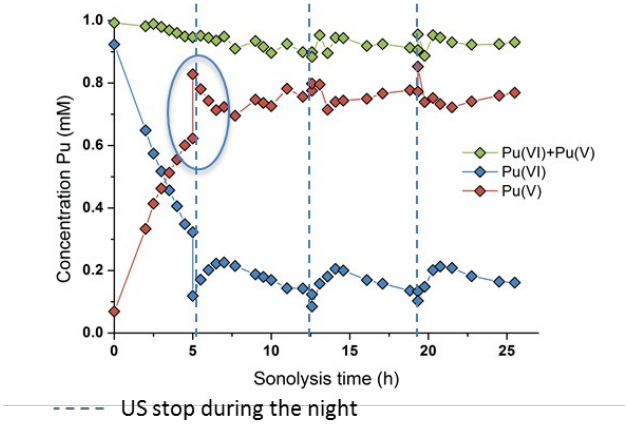

**Figure 3: Behaviour of a 1 mM Pu(VI) solution under low frequency ultrasound (20 kHz, 0.34 W mL$^{-1}$, 21°C, Ar/(20%)$O_2$) as a function of sonolysis time (" ⋮ " symbolizes ultrasound stop during the night; the green data express the sum of the determined concentrations of Pu(VI) and Pu(V)). A solution pH decrease from 3.6 to 2.1 after sonication was observed.**

At 20 kHz, several days were required under Ar/$O_2$ atmosphere to reduce Pu(VI) solutions as evidenced in Figure 3. The plotted measurements indicate that Pu(VI) reduction continue during the night when sonication stops (the absence of ultrasound is notified with dashed lines but the measurements acquired during that time are not showed, Figure 3 only shows data obtained under sonication). Such observation is related to the overproduction of $H_2O_2$ which continue the reduction process without ultrasound in agreement with high frequency experiments. The analyses indicated a $H_2O_2$ concentration of about 1.4 mM after 12.5 h of sonication which decreased to 0.6 mM after night. Another striking observation is the increase of Pu(VI) concentration (with a simultaneous decrease of Pu(V)) when ultrasound starts again. This phenomenon is then followed, after several hours, by a resumption of Pu(VI) reduction which phenomena can be reproduced several times (Figure 3). This phenomenon was not observed under pure Ar atmosphere or during the simple bubbling of Ar/$O_2$ in Pu(V) solutions. This phenomenon can therefore be related to the presence of $O_2$ during sonication. In fact, hydroperoxyl radicals that can be produced during sonication in the presence of $O_2$, are very reactive species which can involve complex reactions with Pu ions. Particularly, radiolysis investigations have showed that Pu(V) can be oxidized by hydroperoxyl radicals in agreement with the reaction (16).[76] We suggest that the sonochemical formation of $HO_2^{\cdot}$ species may involve two competitive reactions that may interfere with Pu(VI) reduction process: $H_2O_2$ formation versus Pu(V) reoxidation. Once a sufficient amount of $H_2O_2$ is produced, Pu(VI) reduction may occur again. Note that under Ar/(10%)CO atmosphere, which allows the scavenging of $OH^{\cdot}$ radicals and prevents $H_2O_2$ formation in agreement with the reaction (17), Pu(VI) reduction is not observed. This confirms again the proposed mechanism involving $H_2O_2$. Furthermore, the pH measured after sonication was found to be about pH = 2.1 (instead of 3.6 before the experiment) which confirms the release of protons during the reduction process (reaction (9)).

$$PuO_2^{+} + HO_2^{\cdot} + H^{+} \rightarrow PuO_2^{2+} + H_2O_2 \quad (16)$$

$$CO + OH^{\cdot} \rightarrow CO_2 + H \quad (17)$$

Generally, the reported ultrasound procedure for Pu(V) preparation agrees with conventional chemistry of Pu reported in the literature but allows the control of the kinetics through the *in situ* generation of active species without addition of any side chemicals (Figures S5 and S6, Supporting Information). It is important to emphasize that under the here described preparation conditions, Pu(V) solutions are quite concentrated and highly pure. Most of the Pu(VI) is reduced into Pu(V) under high frequency ultrasound in few hours; the slight sonochemical overproduction of $H_2O_2$ allows reducing the remaining amount to 1% or less. Whatever the sonication conditions (frequency, atmosphere and concentration), the various Pu(VI) solutions never lead to the observation of Pu(III) or Pu(IV), Pu(IV) colloids, brown or red Pu(IV) peroxo complexes, and Pu(IV) green precipitates.[2, 81]

### 3.2. Stability of the Pu(V) solutions

In the absence of Pu(III) traces in solution, Pu(V) disproportionation has been reported to be strongly dependent to hydrogen ion concentration (reactions (1-2)). Therefore, the stability of the prepared Pu(V) solutions at the laboratory can be explained by their relatively high pH (>2) combined to the

moderate Pu concentration of the solutions in agreement with the literature.[2, 3, 36] Under these conditions, Pu(V) disproportionation rate is very weak. Thermodynamically, Pu(V) can also be reduced by the residual amount of $H_2O_2$ present in solution in agreement with the kinetic law shown below (equation (18)). The rate constant for this reaction was only studied in basic media and was reported to be quite low and reached about 3.59 $10^{-9}$ $min^{-1}$ against 0.75 $min^{-1}$ for Pu(VI) reduction with $H_2O_2$ and 0.24 $M^{-1}$ $min^{-1}$ for Pu(V) disproportionation (at 25°C, 1 M $HClO_4$).[16]

$$-\frac{d[PuO_2^+]}{dt} = k\frac{[Pu(V)][H_2O_2]}{[H^+]} \qquad (18)$$

Figure 4 shows several absorption spectra obtained from Pu(V) solutions prepared at low and high frequency ultrasound illustrating their stabilities during storage under air atmosphere. Note again that some of the freshly prepared solution contained some traces of Pu(VI) observable on the absorption spectrum because of its high molar attenuation coefficient (ε = 533 $cm^{-1}$ $M^{-1}$); but the corresponding concentration represents less than 1% of the Pu content (few hours after sonication). From the spectroscopic measurements it follows that Pu(V) solutions prepared under these conditions are stable during approximately one month whatever the saturating gas atmosphere used during sonolysis (Ar or $Ar/O_2$). However, after approximately one month storage, Pu(VI) concentration slightly increases while Pu(V) amount is found to decrease, most probably through disproportionation. Interestingly, this phenomenon is accompanied by the formation of new absorption peaks standing at 455 nm and 650 nm (large peak) which are currently under investigation and differ from classical Pu(IV) colloids. Pu colloids can indeed be recognized by the presence of an absorption peak around 620 nm and a strong absorption in the near UV range attributed to Mie scattering.[2, 82]

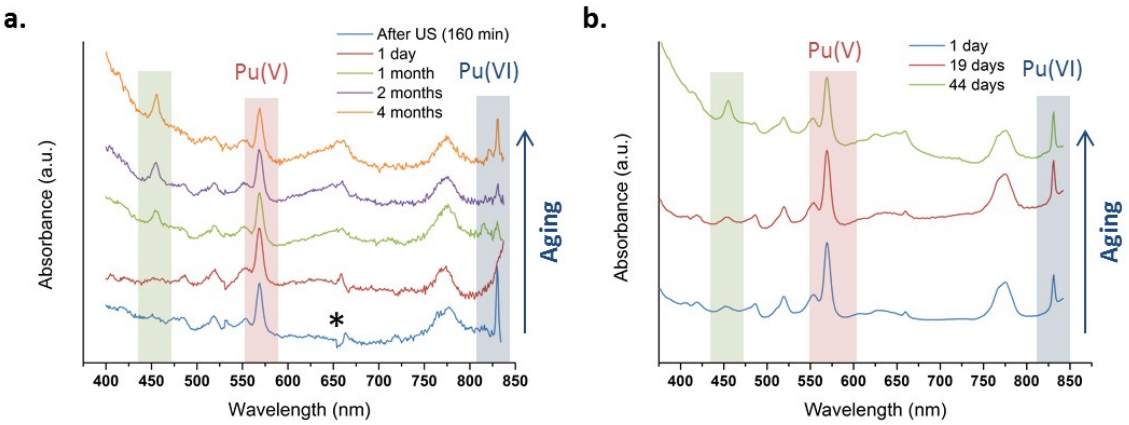


**Figure 4 : UV-vis absorption spectra observed after sonication at 21°C of a Pu(VI) solution at 203 kHz under aerobic atmosphere at (a.) 1 mM with optic fibers, and (b.) 2.3 mM without optic fibers. One day after sonication, the final amount of Pu(VI) is <1% of the Pu content (* is an optical artefact due to optic fibers).**

## 3.3. Characterizations

### *3.3.1. XAFS experiments*

The relative stability and concentration of the prepared Pu(V) solutions allowed us to investigate structural properties by XAFS (which were carried out few days after synthesis). The Pu $L_{III}$-edge X-ray absorption near edge structure (XANES) spectrum of a 1 mM Pu(V) solution prepared with ultrasound is shown in Figure 5.a. together with the reference XANES spectra of Pu(IV) and Pu(VI)

View Article Online
DOI: 10.1039/C7QI00389G

aqua ions. In agreement with the literature,[83] the spectrum of the sonochemical Pu(V) exhibits a decreased white line height in comparison to Pu(IV) and Pu(VI). Moreover, the Pu(V) spectrum shows on its high energy side the same "yl" shoulder as observed for the Pu(VI) reference, which is characteristic for the presence of trans dioxo bounds. Furthermore, the absorption edge of the Pu(V) sample is also found to be shifted to lower energy when compared to Pu(VI), hence confirming the presence of the pentavalent state in the solution.[23, 83] A beat node, typical for trans dioxo actinide species, can be observed between 6 and 8.5 $Å^{-1}$ among the oscillations of the real part of the $k^3$-weighted EXAFS spectra (Figure 5.b., insert). Two large peaks standing at 1.38 Å and 1.9 Å (uncorrected for phase-shift) can be observed in the Fourier transform (FT) of the $k^3$-weighted interval 2 $Å^{-1}$ < k < 12.3 $Å^{-1}$ (Figure 5.b.) which indicate the presence of two well-defined coordination shells.

The peak standing at R+ϕ = 1.38 Å corresponds to the scattering contribution of the Pu-$O_{yl}$, distances whereas the peak observed on the FT spectra at R+ϕ = 1.9 Å can be attributed to the scattering contribution of O stemming from coordinated $H_2O$ molecules. Theoretical EXAFS simulations confirmed the presence of two oxo moieties at 1.81 Å and 5.3 $H_2O$ molecules at 2.47 Å in the equatorial plane. These structural parameters are in line with those generally observed for the pentavalent state of Pu in non-complexing media although a lower coordination number has been reported for the equatorial solvation environment, notably with XAFS.[21-23, 83] In agreement with the work of Ikeda-Ohno *et al.* dedicated to the complexation behavior of Np ions in aqueous solutions,[28] we observed that $PuO_2^+$ EXAFS spectra can be simulated with very good fitting residues (R-factor < 2%) and appropriate $\sigma^2$ leading to a coordination number ranging from N[$O_{eq}(H_2O)$] = 4 to 6. The results are summarized in Figure S7 (Supporting Information) and compared with literature data related to $PuO_2^+$ and $NpO_2^+$ first solvation shell in aqueous non-complexing media. As suggested by this Figure, the determination of the exact number of water molecules coordinating the ion in the equatorial plane with only EXAFS technique may suffer from large errors. There appears to be from the literature a general consensus that the coordination environment of Np(V) equal to N[$O_{eq}(H_2O)$] = 5 whereas the hydration number of $PuO_2^+$ is still a matter of discussion.[19-21, 28, 73, 84, 85] A more relevant approach was therefore considered by simulating EXAFS signal from $PuO_2^+$ complexes generated with 4 or 5 coordinating water molecules in the equatorial plane by DFT calculations with optimized geometries and vibrational frequencies.

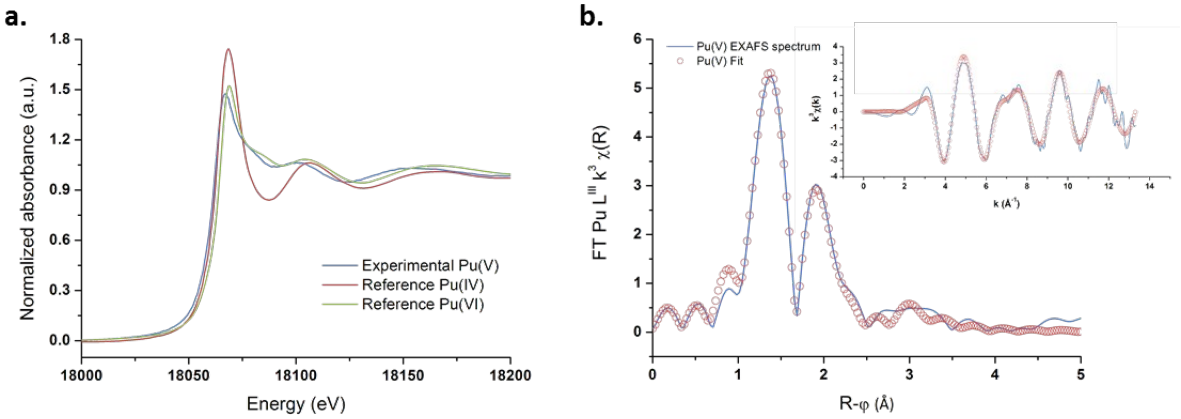


**Figure 5: (a.) XANES spectrum obtained for ultrasound prepared Pu(V) (203 kHz, 20°C, 0.13 W $mL^{-1}$) and reference spectra of pure Pu(VI) and Pu(IV). (b.) FT of the experimental $k^3$-weighted EXAFS spectrum of Pu(V) and theoretical EXAFS spectrum obtained by the shell fit. Insert: Experimental and fitted EXAFS spectra of sonochemical Pu(V).**

View Article Online
DOI: 10.1039/C7QI00389G

**Table 1: EXAFS structural parameters calculated from $k^3$-weighted EXAFS spectra for the sonochemical Pu(V) and its comparison with literature data. R-factor +1.7% *Fixed value, $S_0^2$ = 0.8. CN: coordination number, R: interatomic distance, $\sigma^2$: Debye-Waller factor, $\Delta E_0$: threshold energy. The standard deviations of the variable parameters estimated by the IFEFFIT software are given in parentheses.[56, 57]**

| Atom | N | R(Å) | $\sigma^2$ / Å² | $\Delta E_0$ | Ref. |
|---|---|---|---|---|---|
| **$O_{yl}$** | **2.0*** | **1.81(1)** | **0.002(1)** | **2.38(5)** | **This work** |
| **$O_{eq}$** | **5.3(1.0)** | **2.47(2)** | **0.009(1)** | **2.38(5)** | |
| $O_{yl}$ | 2.0* | 1.821 (5) | 0.001 | - | Panak et al.[22] |
| $O_{eq}$ | 3.8 (4) | 2.48 (1) | 0.005 | - | |
| $O_{yl}$ | 2.0* | 1.81(1) | 0.002 | - | Di Giandomenico *et al.*[21] |
| $O_{eq}$ | 3.3(8) | 2.47(2) | 0.004 | - | |
| $O_{yl}$ | 2.0* | 1.81 | - | - | Conradson *et al.*[23] |
| $O_{eq}$ | 4 | 2.47 | - | - | |

*N for Pu-$O_{ax}$ is fixed at 2.0.

### *3.3.2. DFT calculations*

$PuO_2(H_2O)_4(H_2O)_8^+$ and $PuO_2(H_2O)_5(H_2O)_{10}^+$ aqua complexes with respectively four and five inner shell water molecules were considered in the DFT calculations (with optimized geometries and vibrational frequencies) and the corresponding EXAFS spectra were simulated in an attempt to discriminate the solvation shell of $PuO_2^+$ aqua ion. In the complexes, two outer-shell water molecules are hydrogen bonded to each inner shell molecule. Preliminary studies focused on the uranyl aqua ion confirmed that the structural parameters of the aqua ion can be correctly reproduced by such DFT calculations (see the experimental part). For both plutonyl complexes, the structural parameters are provided in Table 2 and the theoretical EXAFS spectra are compared to the experimental one in Figure 6. The simulated spectrum for $PuO_2(H_2O)_4(H_2O)_8^+$ is in very good agreement with the experimental signal while a poor agreement is found for $PuO_2(H_2O)_5(H_2O)_{10}^+$. For $PuO_2(H_2O)_4(H_2O)_8^+$, two well-defined shell attributed to dioxo bonds and Pu-$O_{eq}$ interactions can be observed in agreement with XAFS experiments. For $PuO_2(H_2O)_5(H_2O)_{10}^+$, the second FT peak observed experimentally at R+ϕ = 1.9 Å is split into two on the FT derived from the calculated spectrum. Calculated Pu-O distances and Debye-Waller factors compares very well with experimental distances when considering $PuO_2^+$ complex with four inner shell water molecules. The calculated and experimental Pu-$O_{yl}$ and Pu-$O_{eq}$ distances agree within 0.02 Å.

Calculated Debye-Waller factors are equal to those reported by Panak *et al*. which is consistent with the good match found between simulated and experimental EXAFS signal.[22] For the $PuO_2^+$ complex with five inner shell water molecules, the strong Pu-$O_{yl}$ bond remains equal to 1.80 Å and are not altered by the number of coordinating water molecule. By contrast, the value calculated for the Pu-$O_{eq}$ average bond length is significantly too long by 0.08-0.09 Å to fit with the experimental results. Because of steric crowding in the inner shell, one Pu-$O_{eq}$ distance is elongated. Accordingly, the calculated Debye-Waller factors associated with Pu-$O_{eq}$ increase since the Pu-$O_{eq}$ bond are becoming weaker than in $PuO_2(H_2O)_4(H_2O)_8^+$. To summarize, the very good agreement found with both the calculated and experimental data for the tetra-aqua $PuO_2^+$ complex strongly supports that it is the predominant $PuO_2^+$ specie in aqueous non-complexing media.

View Article Online
DOI: 10.1039/C7QI00389G

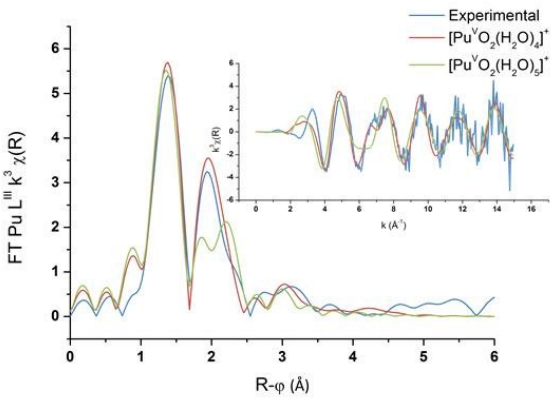


**Figure 6: Ab initio and experimental Pu $L_{III}$-edge $k^3$-weighted EXAFS spectra (inset) and the corresponding Fourier transforms of Pu(V) aqua ion, and ab initio spectra for $PuO_2(H_2O)_4(H_2O)_8^+$ (red) and $PuO_2(H_2O)_5(H_2O)_{10}^+$ (green).**

**Table 2: Average values for DFT (B3LYP) structural parameters calculated for $PuO_2(H_2O)_4(H_2O)_8^+$ and $PuO_2(H_2O)_5(H_2O)_{10}^+$ complexes, interatomic distances (R) and Debye-Waller factor ($\sigma^2$).**

| Model | Atom | N | R(Å) | $\sigma^2$ / Å² |
|---|---|---|---|---|
| $PuO_2(H_2O)_4(H_2O)_8^+$ | $O_{yl}$ | 2 | 1.800 | 0.0015 |
| | $O_{eq}$ | 4 | 2.480 | 0.0051 |
| $PuO_2(H_2O)_5(H_2O)_{10}^+$ | $O_{yl}$ | 2 | 1.801 | 0.0015 |
| | $O_{eq}$ | 5 | 2.561* | 0.0073 |

* Pu-O distances are split into two groups of distances: 4 Pu-O at 2.54 Å and 1 Pu-O at 2.64 Å

### *3.3.3. Magnetic susceptibility*

NMR measurements were performed by the Evans method on several Pu(V) solutions (Figure S8, Supporting Information).[74, 86] Particularly, the Pu(V) solution was concentrated by dry Ar bubbling overnight (3.8 mM) to provide a better signal intensity for some experiments. Figure 7 illustrates the averaged paramagnetic behaviour of Pu(V) investigated in the 5-50°C temperature range. To evaluate the accuracy of the measurements, the stability of the solution towards redox transformations during NMR analyses has been followed by UV-Visible absorption spectroscopy (Figure 7 inset) before and after analysis. Before NMR measurements, only traces of Pu(VI) can be noticed in the Pu(V) solution (no other oxidation states or species are observed). Such pollution corresponds to a Pu(VI) concentration of 66 µM which represents less than 1.7% of the total Pu content in the solution. After NMR analyses, the Pu(VI) content is estimated at about 30 µM (0.8% of the total Pu content). The amount of Pu(VI) engaged in the analysed solutions appears nevertheless too low to induce a significant variation of the NMR signal. No other Pu oxidation states or species is observed on these spectra emphasizing the accuracy of the obtained results despite the slight variations observed with the magnetic susceptibility values. It is also important to note that potential traces of hydrogen peroxide resulting from sonication are assumed to not interfere with NMR signal in agreement with the literature.[87]

The plotted molar magnetic susceptibilities (Figure 7) can be fitted with a linear regression in agreement with a Curie-like law ($\chi^{-1}$ linear with T); the slope of this regression gives a Curie constant of about 6.896 $10^{-6}$ $m^3$.K.$mol^{-1}$. In comparison to the other Pu oxidation states measured in perchloric solutions (Table 3), the experimental value measured at 25°C for Pu(V) magnetic susceptibility ($\chi_M$ =

View Article Online
DOI: 10.1039/C7QI00389G

16.3 $10^{-9}$ $m^3mol^{-1}$) is situated between the ones measured for Pu(III) and Pu(IV) ($\chi_M$ = 4.7 $10^{-9}$ and 28.4 $10^{-9}$ $m^3mol^{-1}$, respectively;[18, 88] Pu(VI) is much higher).[17] Nevertheless, Pu(V) susceptibility is lower than the predicted value for the free ion taking into account the ground state J = 9/2 only ($\chi_M$ about 70 $10^{-9}$ $m^3mol^{-1}$) and even lower than the one reported for Np(IV) ($\chi_M$ = 48.6 $10^{-9}$ $m^3mol^{-1}$) which exhibits the same isoelectronic $5f^3$ configuration.[18] The observed difference between Np(IV) and Pu(V) ions supports the current investigations related to the development of theoretical models dedicated to the study of the magnetic susceptibility shifts as a function of the electronic configuration.

**Table 3: Comparison of the magnetic susceptibility ($\chi_M$) of some Pu and Np ions experimentally measured at 25°C in perchloric media.**

| Specie | $\chi_M$ ($10^{-9}$ $m^3mol^{-1}$) | Ref. |
|---|---|---|
| Pu(III) | 4.7 | Autillo *et al.*[88] |
| Pu(IV) | 28.4 | Autillo *et al.*[18] |
| **Pu(V)** | **16.3** | **This work** |
| Np(IV) | 48.6 | Autillo *et al.*[18] |

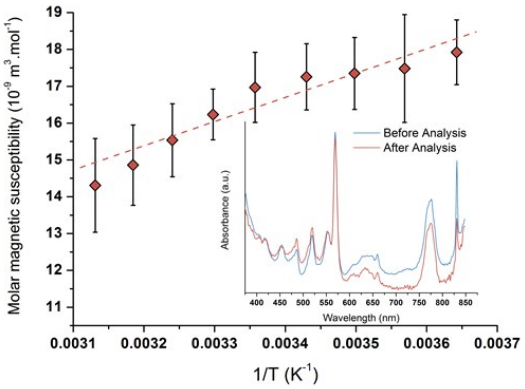


**Figure 7: Molar magnetic susceptibility as a function of 1/T averaged for different Pu(V) solutions ($R^2$= 0.96). UV-Visible absorption spectra obtained for a 3.8 mM Pu(V) solution before and after NMR experiments showing the absence of modification of the Pu oxidation states excepted a small decrease of Pu(VI) amount (respectively in blue and red).**

## 4. Conclusions

This work describes a facile and original sonochemical method for the preparation of Pu(V) solutions free from the admixture of other oxidation states of plutonium. At the studied conditions, Pu(VI) reduction occurs through the ultrasonically triggered generation of $H_2O_2$ in water which can be dramatically enhanced under $Ar/O_2$ atmosphere and high-frequency ultrasound (203 kHz). Ultrasonic irradiation allows Pu(VI) reduction without the addition of any side chemicals and avoids dilutions often correlated to hydrolysis issues. The prepared Pu solutions are at the millimolar range and are quasi-exclusively composed of Pu(V). Traces of Pu(VI) in the range of the percent can eventually pollute the prepared solutions which were found to be stable for almost one month. Such conditions allowed the solutions to be characterized by XANES and EXAFS spectroscopies which confirmed the presence of the Pu(V) aqua ion in agreement with the literature. The solvation environment of the $PuO_2^+$ aqua complex was clarified by simulating EXAFS spectra from optimized $PuO_2^+$ structures generated from DFT calculations which evidenced that the tetra-aqua complex $[Pu^VO_2(H_2O)_4(H_2O)_8]^+$

View Article Online
DOI: 10.1039/C7QI00389G

dominates in aqueous non complexing media. For the first time, NMR measurements were enabled for Pu(V) which allowed us to determine its magnetic susceptibility ($\chi_M$ = 16.3 $10^{-9}$ $m^3mol^{-1}$ at 25°C) and Curie constant (C = 6.896 $10^{-6}$ $m^3.K.mol^{-1}$). Generally, this work provides an original approach for Pu(V) preparation which contributes in supplying new insights regarding its structure and magnetic properties. The preparation of more concentrated Pu(V) solutions is in progress and should improve the accuracy of future investigations.

## Acknowledgments

The authors acknowledge French CEA/DEN for the financial support. Our special thanks to M. Guigue, J. Vermeulen, and G. Maurin for their help in experiments.

## References

1. S. W. Rabideau and R. J. Kline, *J. Phys. Chem.*, 1958, **62**, 617-620.
2. D. Clark, S. Hecker, G. Jarvinen and M. Neu, in *The Chemistry of the Actinide and Transactinide Elements*, eds. L. Morss, N. Edelstein and J. Fuger, Springer Netherlands, 2011, DOI: 10.1007/978-94-007-0211-0_7, ch. 7, pp. 813-1264.
3. W. Newton, *The kinetics of the oxidation-reduction reactions of uranium, neptunium, plutonium, and americium in solutions*, Report TID-26506, Los Alamos Scientific Laboratory, 1975.
4. V. Neck, M. Altmaier, A. Seibert, J. I. Yun, C. M. Marquardt and T. Fanghanel, *Radiochim. Acta*, 2007, **95**, 193-207.
5. S. Topin and J. Aupiais, *J. Environ. Radioact.*, 2016, **153**, 237-244.
6. K. A. Orlandini, W. R. Penrose and D. M. Nelson, *Mar. Chem.*, 1986, **18**, 49-57.
7. W. R. Penrose, D. N. Metta, J. M. Hylko and L. A. Rinckel, *J. Environ. Radioact.*, 1987, **5**, 169-184.
8. W. R. Penrose, W. L. Polzer, E. H. Essington, D. M. Nelson and K. A. Orlandini, *Environ. Sci. Technol.*, 1990, **24**, 228-234.
9. W. L. Keeney-Kennicutt and J. W. Morse, *Geochim. Cosmochim. Acta*, 1985, **49**, 2577-2588.
10. G. T. Seaborg, J. J. Katz and W. M. Manning, *The Transuranium Elements: Research Papers*, New York: McGraw-Hill Book Co., Inc., 1949.
11. R. E. Connick, *J. Am. Chem. Soc.*, 1949, **71**, 1528-1533.
12. A. L. Sanchez, J. W. Murray and T. H. Sibley, *Geochim. Cosmochim. Acta*, 1985, **49**, 2297-2307.
13. M. P. Neu, D. C. Hoffman, K. E. Roberts, H. Nitsche and R. J. Silva, *Radiochim. Acta*, 1994, **66-7**, 251-258.
14. N. A. Conroy, E. M. Wylie and B. A. Powell, *Anal. Chem.*, 2016, **88**, 4196-4199.
15. D. Cohen, *J. Inorg. Nucl. Chem.*, 1961, **18**, 207-210.
16. S. W. Rabideau, *J. Am. Chem. Soc.*, 1957, **79**, 6350-6353.
17. T. F. Wall, S. Jan, M. Autillo, K. L. Nash, L. Guerin, C. Le Naour, P. Moisy and C. Berthon, *Inorg. Chem.*, 2014, **53**, 2450-2459.
18. M. Autillo, L. Guerin, D. Guillaumont, P. Moisy, H. Bolvin and C. Berthon, *Inorg. Chem.*, 2016, **55**, 12149-12157.
19. K. E. Knope and L. Soderholm, *Chem. Rev.*, 2013, **113**, 944-994.
20. M. R. Antonio, L. Soderholm, C. W. Williams, J. P. Blaudeau and B. E. Bursten, *Radiochim. Acta*, 2001, **89**, 17-25.
21. M. V. Di Giandomenico, C. Le Naour, E. Simoni, D. Guillaumont, P. Moisy, C. Hennig, S. D. Conradson and C. Den Auwer, *Radiochim. Acta*, 2009, **97**, 347-353.

22. P. J. Panak, C. H. Booth, D. L. Caulder, J. J. Bucher, D. K. Shuh and H. Nitsche, *Radiochim. Acta*, 2002, **90**, 315-321.
23. S. D. Conradson, K. D. Abney, B. D. Begg, E. D. Brady, D. L. Clark, C. den Auwer, M. Ding, P. K. Dorhout, F. J. Espinosa-Faller, P. L. Gordon, R. G. Haire, N. J. Hess, R. F. Hess, D. W. Keogh, G. H. Lander, A. J. Lupinetti, L. A. Morales, M. P. Neu, P. D. Palmer, P. Paviet-Hartmann, S. D. Reilly, W. H. Runde, C. D. Tait, D. K. Veirs and F. Wastin, *Inorg. Chem.*, 2004, **43**, 116-131.
24. S. D. Conradson, *Appl. Spectrosc.*, 1998, **52**, 252A-279A.
25. S. Tsushima and A. Suzuki, *J. Mol. Struct. THEOCHEM*, 2000, **529**, 21-25.
26. A. Y. Garnov, N. N. Krot, A. A. Bessonov and V. P. Perminov, *Radiochemistry*, 1996, **38**, 402-406.
27. P. J. Hay, R. L. Martin and G. Schreckenbach, *J. Phys. Chem. A*, 2000, **104**, 6259-6270.
28. A. Ikeda-Ohno, C. Hennig, A. Rossberg, H. Funke, A. C. Scheinost, G. Bernhard and T. Yaita, *Inorg. Chem.*, 2008, **47**, 8294-8305.
29. S. O. Odoh, E. J. Bylaska and W. A. de Jong, *J. Phys. Chem. A*, 2013, **117**, 12256-12267.
30. A. E. Clark, A. Samuels, K. Wisuri, S. Landstrom and T. Saul, *Inorg. Chem.*, 2015, **54**, 6216-6225.
31. V. S. Koltunov, I. A. Kulikov, N. V. Kermanova and L. K. Nikishova, *Sov. Radiochem.*, 1981, **23**, 384-386.
32. G. A. Fugate and J. D. Navratil, in *Separations for the Nuclear Fuel Cycle in the 21st Century*, eds. G. J. Lumetta, K. L. Nash, S. B. Clark and J. I. Friese, American Chemical Society, Washington, 2006, vol. 933, pp. 167-181.
33. V. I. Marchenko, K. N. Dvoeglazov and V. I. Volk, *Radiochemistry*, 2009, **51**, 329-344.
34. S. F. Marsh and T. D. Gallegos, *Chemical treatment of plutonium with hydrogen peroxide before nitrate anion exchange processing. [Reduction to (IV)]*, Report LA-10907, 1987.
35. A. J. Bard, R. Parsons and J. Jordan, *Standard Potentials in Aqueous Solution*, Taylor & Francis, 1985.
36. C. Maillard and J. M. Adnet, *Radiochim. Acta*, 2001, **89**, 485-490.
37. S. I. Nikitenko, L. Venault, R. Pflieger, T. Chave, I. Bisel and P. Moisy, *Ultrason. Sonochem.*, 2010, **17**, 1033-1040.
38. M. Virot, L. Venault, P. Moisy and S. I. Nikitenko, *Dalton Trans.*, 2015, **44**, 2567-2574.
39. T. J. Mason and J. P. Lorimer, *Applied sonochemistry, The uses of power ultrasound in chemistry and processing*, Weinheim, 2002.
40. K. Makino, M. M. Mossoba and P. Riesz, *J. Am. Chem. Soc.*, 1982, **104**, 3537-3539.
41. K. Makino, M. M. Mossoba and P. Riesz, *J. Phys. Chem.*, 1983, **87**, 1369-1377.
42. E. J. Hart and A. Henglein, *J. Phys. Chem.*, 1985, **89**, 4342-4347.
43. C. H. Fischer, E. J. Hart and A. Henglein, *J. Phys. Chem.*, 1986, **90**, 1954-1956.
44. C. H. Fischer, E. J. Hart and A. Henglein, *J. Phys. Chem.*, 1986, **90**, 222-224.
45. E. L. Mead, R. G. Sutherland and R. E. Verrall, *Can. J. Chem.*, 1976, **54**, 1114-1120.
46. C. Petrier, A. Jeunet, J. L. Luche and G. Reverdy, *J. Am. Chem. Soc.*, 1992, **114**, 3148-3150.
47. M. A. Beckett and I. Hua, *J. Phys. Chem.*, 2001, **105**, 3796-3802.
48. N. M. Navarro, T. Chave, P. Pochon, I. Bisel and S. I. Nikitenko, *J. Phys. Chem. B*, 2011, **115**, 2024-2029.
49. R. Pflieger, T. Chave, G. Vite, L. Jouve and S. I. Nikitenko, *Ultrason. Sonochem.*, 2015, **26**, 169-175.
50. E. Dalodière, M. Virot, P. Moisy and S. I. Nikitenko, *Ultrason. Sonochem.*, 2016, **29**, 198-204.
51. I. Hua and M. R. Hoffmann, *Environ. Sci. Technol.*, 1997, **31**, 2237-2243.
52. P. R. Gogate, A. M. Wilhelm and A. B. Pandit, *Ultrason. Sonochem.*, 2003, **10**, 325-330.
53. T. Chave, N. M. Navarro, S. Nitsche and S. I. Nikitenko, *Chem-Eur J*, 2012, **18**, 3879-3885.
54. T. J. Mason, *Practical sonochemistry: user's guide to applications in chemistry and chemical engineering*, E. Horwood, 1991.
55. W. Matz, N. Schell, G. Bernhard, F. Prokert, T. Reich, J. Claussner, W. Oehme, R. Schlenk, S. Dienel, H. Funke, F. Eichhorn, M. Betzl, D. Prohl, U. Strauch, G. Huttig, H. Krug, W. Neumann,

V. Brendler, P. Reichel, M. A. Denecke and H. Nitsche, *J. Synchrotron Rad.*, 1999, **6**, 1076-1085.
56. B. Ravel and M. Newville, *J. Synchrotron Rad.*, 2005, **12**, 537-541.
57. B. Ravel and M. Newville, *Phys. Scr.*, 2005, 1007-1010.
58. J. J. Rehr and R. C. Albers, *Rev. Mod. Phys.*, 2000, **72**, 621-654.
59. W. Kuchle, M. Dolg, H. Stoll and H. Preuss, *J. Chem. Phys.*, 1994, **100**, 7535-7542.
60. X. Y. Cao, M. Dolg and H. Stoll, *J. Chem. Phys.*, 2003, **118**, 487-496.
61. X. Y. Cao and M. Dolg, *J. Mol. Struct. THEOCHEM*, 2004, **673**, 203-209.
62. M. J. Frisch, *Gaussian 09*, Wallingford, CT, 2009.
63. E. Acher, Y. H. Cherkaski, T. Dumas, C. Tamain, D. Guillaumont, N. Boubals, G. Javierre, C. Hennig, P. L. Solari and M. C. Charbonnel, *Inorg. Chem.*, 2016, **55**, 5558-5569.
64. E. Acher, T. Dumas, C. Tamain, N. Boubals, P. L. Solari and D. Guillaumont, *Dalton Trans.*, 2017, **46**, 3812-3815.
65. J. J. Rehr, J. J. Kas, F. D. Vila, M. P. Prange and K. Jorissen, *Phys. Chem. Chem. Phys.*, 2010, **12**, 5503-5513.
66. F. D. Vila, V. E. Lindahl and J. J. Rehr, *Phys. Rev. B*, 2012, **85**.
67. J. Neuefeind, L. Soderholm and S. Skanthakumar, *J. Phys. Chem. A*, 2004, **108**, 2733-2739.
68. B. Siboulet, C. J. Marsden and P. Vitorge, *Chem. Phys.*, 2006, **326**, 289-296.
69. K. E. Gutowski and D. A. Dixon, *J. Phys. Chem. A*, 2006, **110**, 8840-8856.
70. L. Semon, C. Boehme, I. Billard, C. Hennig, K. Lutzenkirchen, T. Reich, A. Rossberg, I. Rossini and G. Wipff, *ChemPhysChem*, 2001, **2**, 591-598.
71. H. A. Thompson, G. E. Brown and G. A. Parks, *Am. Mineral.*, 1997, **82**, 483-496.
72. U. Wahlgren, H. Moll, I. Grenthe, B. Schimmelpfennig, L. Maron, V. Vallet and O. Gropen, *J. Phys. Chem. A*, 1999, **103**, 8257-8264.
73. P. G. Allen, J. J. Bucher, D. K. Shuh, N. M. Edelstein and T. Reich, *Inorg. Chem.*, 1997, **36**, 4676-4683.
74. D. F. Evans, *J. Chem. Soc.*, 1959, 2003-2005.
75. R. J. Wood, J. Lee and M. J. Bussemaker, *Ultrason. Sonochem.*, 2017, **38**, 351-370.
76. B. Lesigne, PhD thesis, Centre d'études nucléaires de Fontenay-aux-Roses, 1967.
77. G. A. Fugate and J. D. Navratil, in *Acs Sym Ser*, American Chemical Society, 2006, vol. 933, ch. 11, pp. 167-181.
78. S. Merouani, H. Ferkous, O. Hamdaoui, Y. Rezgui and M. Guemini, *Ultrason. Sonochem.*, 2015, **22**, 51-58.
79. J. Lee, M. Ashokkumar, S. Kentish and F. Grieser, *J. Am. Chem. Soc.*, 2005, **127**, 16810-16811.
80. A. A. Ndiaye, R. Pflieger, B. Siboulet, J. Molina, J. F. Dufreche and S. I. Nikitenko, *J. Phys. Chem. A*, 2012, **116**, 4860-4867.
81. R. E. Connick and W. H. Mcvey, *J. Am. Chem. Soc.*, 1949, **71**, 1534-1542.
82. E. Dalodière, M. Virot, V. Morosini, T. Chave, T. Dumas, C. Hennig, T. Wiss, O. Dieste Blanco, D. K. Shuh, T. Tyliszcak, L. Venault, P. Moisy and S. I. Nikitenko, *Sci. Rep.*, 2017, **7:43514**, 1-10.
83. S. D. Conradson, I. Al Mahamid, D. L. Clark, N. J. Hess, E. A. Hudson, M. P. Neu, P. D. Palmer, W. H. Runde and C. Drew Tait, *Polyhedron*, 1998, **17**, 599-602.
84. J. M. Combes, C. J. Chisholmbrause, G. E. Brown, G. A. Parks, S. D. Conradson, P. G. Eller, I. R. Triay, D. E. Hobart and A. Meijer, *Environ. Sci. Technol.*, 1992, **26**, 376-382.
85. T. Reich, G. Bernhard, G. Geipel, H. Funke, C. Hennig, A. Rossberg, W. Matz, N. Schell and H. Nitsche, *Radiochim. Acta*, 2000, **88**, 633-637.
86. K. De Buysser, G. G. Herman, E. Bruneel, S. Hoste and I. Van Driessche, *Chem. Phys.*, 2005, **315**, 286-292.
87. M. Autillo, P. Kaden, A. Geist, L. Guerin, P. Moisy and C. Berthon, *Phys. Chem. Chem. Phys.*, 2014, **16**, 8608-8614.
88. M. Autillo, L. Guerin, H. Bolvin, P. Moisy and C. Berthon, *Phys. Chem. Chem. Phys.*, 2016, **18**, 6515-6525.

View Article Online
DOI: 10.1039/C7QI00389G